X-ray diffuse scattering study of local distortions in $Fe_{1+x}Te$ induced by excess Fe

X. Liu, C.-C. Lee, Z. J. Xu, J. S. Wen, G. Gu, W. Ku, J. M. Tranquada, and J. P. Hill
Condensed Matter Physics and Materials Science Department, Brookhaven National Laboratory, Upton, New York 11973, USA
(Received 19 January 2011; revised manuscript received 7 April 2011; published 31 May 2011)

We report x-ray diffuse scattering studies of the iron chalcogenide $Fe_{1+x}Te$ as a function of doping and temperature for $x = 0.03$, 0.08, and 0.12. In all cases, remarkably strong, characteristic diffuse scattering is observed. This scattering extends throughout the Brillouin zone and exhibits a nonmonotonic decay away from the fundamental Bragg peaks, with a peaklike structure at a reduced $q \approx (0.3,0,0.6)$. We interpret this scattering as Huang diffuse scattering resulting from distortions induced by the interaction between the excess Fe and the FeTe layers. The form of the scattering indicates that this interaction is strong and extends a number of unit cells away from the interstitial Fe site. Further, the diffuse scattering shows a sudden decrease on cooling through the structural and magnetic phase transition, reflecting the first-order change of the electronic structure of FeTe.

DOI: 10.1103/PhysRevB.83.184523 PACS number(s): 61.05.cp, 74.81.−g, 74.70.Dd

Among the recently discovered Fe-based superconducting families, the iron chalcogenide, Fe_{1+x}(Te,Se) family has perhaps the simplest crystal structure. It consists of vertically stacked, tetrahedrally coordinated Fe-Te(Se) sheets which are isostructural to the Fe-As sheets in the pnictides, but without the complicating intervening charge reservoir layers. Theoretical calculations[1] for the stoichiometric iron chalcogenides, FeTe and FeSe, show that the electronic structure and Fermi surface topology are very similar to the pnictides. Indeed, the end member $Fe_{1+x}Te$ shares much in common with the parent compounds of the pnictides; both are tetragonal and paramagnetic at room temperature, and become antiferromagnetically ordered (with different ordering wave vectors) at low temperatures following combined structural and magnetic phase transitions.[2,3] Thus, comparing the two families can help obtain a unified picture of the physics of the iron-based superconductors. However, it is known that a certain amount of excess Fe is required to crystallize $Fe_{1+x}Te$,[2,4] and the presence of this excess Fe complicates the picture in ways that may be far from trivial.

It is believed that the excess Fe goes into the so-called Fe2 site,[2] which is equivalent to the site occupied by Li in LiFeAs.[5] The requirement that excess Fe be present for successful crystal growth indicates that it has a significant impact on the crystal structure. Further, density-functional calculations[6] suggest that the excess Fe is also electronically active—acting as an electron donor, and that it has a large magnetic moment($\sim 2.4\mu_B$) which couples to the Fe in the FeTe layers. Direct evidence for the effect of the excess Fe on the magnetic properties comes from the fact that the antiferromagnetic (AF) ordering temperature T_N and the incommensurability of the AF ordering wave vector may both be tuned by varying the excess Fe concentration.[3] Also, it has been shown that excess Fe is correlated with the suppression of superconductivity and a modification of the dynamic spin correlations.[7] Finally, the importance of the excess Fe has also been hinted at by many other less direct measurements.[8–10]

Despite its importance however, direct experimental observation of the interaction of the excess Fe with the FeTe layers is lacking. In large part, this is because it is difficult to probe the excess Fe directly, since it is a minority species, relative to the Fe1 sites in the FeTe layers. However, the excess Fe, which pulls the system away from perfect stoichiometry and interacts with the FeTe layers, should drive the crystal away from perfect periodicity and will, therefore, give rise to diffuse intensity that may be observed in a scattering experiment. The intensity, momentum dependence, and temperature dependence of such scattering would then probe the response of the FeTe layers to the presence of the excess Fe. Furthermore, one can think of the excess Fe as an internal probe, and studying the response of the FeTe layers to this probe can shed light on the intrinsic electronic properties of this material. As we shall see later, this is in fact the case.

Here, we report such single crystal x-ray diffuse scattering measurements of $Fe_{1+x}Te$ as a function of temperature and excess Fe concentration. We find a characteristic, strong diffuse scattering pattern for all samples studied. We attribute this to Huang diffuse scattering (HDS)[11] arising from large distortions induced by the Fe interstitials. The observed unusual HDS pattern suggests that the interactions between the Fe2 and the FeTe layers extend across a few unit cells rather than being confined to the nearest neighbors. This in turn is indicative of a strong response of the FeTe lattice to perturbation by the excess Fe. In addition, we find that the interaction strength decreases abruptly at T_N as the low temperature AF ordered state is entered. This can be explained by the first-order change of the electronic structure of FeTe.

The $Fe_{1+x}Te$ samples studied here were grown via the unidirectional solidification method. Samples with different excess Fe concentration, namely, $x = 0.03$,0.08, and 0.12, were studied. The experiments were carried out at beamline X22C at the National Synchrotron Light Source. All samples were cleaved in air and immediately sealed in the vacuum of a closed cycle refrigerator. The data are normalized by the iron fluorescence intensity which accounts for the angular dependence of the effective scattering volume.

Figure 1 shows the two-dimensional diffuse scattering patterns from the $Fe_{1.03}Te$ and $Fe_{1.12}Te$ samples, collected in the $(H\ 0\ L)$ plane around the Bragg peaks [0 0 7] and [±1 0 6] at $T = 20$ K. Since the measured intensity was found to be inversion symmetric about the Bragg peaks, only half of the HDS pattern around the individual Bragg peaks is presented.

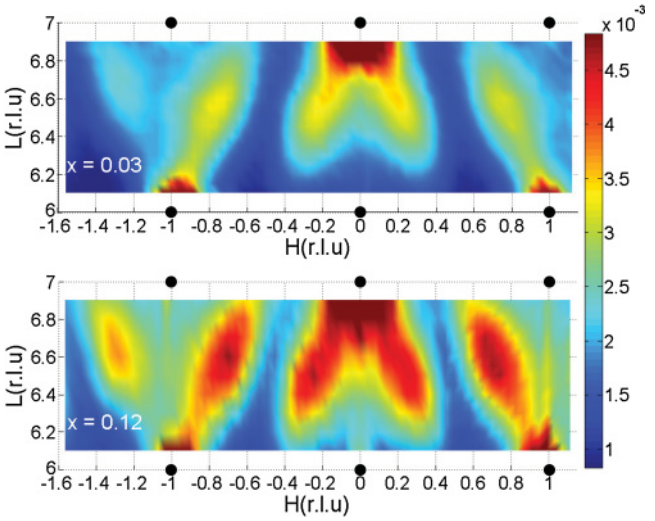

FIG. 1. (Color online) X-ray diffuse scattering pattern measured in the (H 0 L) plane from (Top panel) $Fe_{1.03}Te$ and (Bottom panel) $Fe_{1.12}Te$ at $T = 20$ K.

Interestingly, even though the larger excess Fe concentration gives rise to a higher intensity, the diffuse scattering from both samples has a similar characteristic momentum dependence.

There are two striking aspects to the HDS scattering in Fig. 1 which allow us to draw conclusions immediately without any need for quantitative analysis. First, the HDS intensities are surprisingly strong. To appreciate the intensity of the diffuse scattering from $Fe_{1+x}Te$, we compare our result with that observed at low temperatures from cuprates, where lattice strain is induced by oxygen vacancies[12] or substitutions.[13] In these cuprate systems, the HDS intensities show a monotonic decrease in intensity away from the Bragg peaks and decrease into the thermal diffuse scattering background quickly within less than half the Brillouin zone. In striking contrast, the data for $Fe_{1+x}Te$ show HDS ridges that extend across the full Brillouin zone and into the nearby zones. Even at $L = 6.1(6.9)$, the HDS tails extending from [0 0 7] ([±1 0 6]) are still quite pronounced. To our knowledge, HDS of this strength has only been reported before in one case for strongly correlated systems, namely, the colossal magnetoresistive(CMR) manganite $La_{1.2}Sr_{1.8}Mn_2O_7$.[14] In the manganite case, it is believed that the HDS originates from a Jahn-Teller(JT) distortion, and, in fact, this distortion is key to determining the electronic properties of such CMR materials.

The second striking feature is that the diffuse scattering shows a modulated structure rather than the simple monotonic decrease, common to the other systems mentioned above. In particular, there is a peaklike feature at total momentum transfer $\mathbf{Q} \approx (\pm 0.3, 0, \pm 0.6) + \mathbf{G}$, where $\mathbf{G}$ is a reciprocal lattice point. This nonmonotonic behavior is very clear for the ridges extending from [±1 0 6]. It is not as pronounced at this color scale for the ridges extending from [0 0 7] because the overall intensities around [0 0 7] are much higher. Such nonmonotonic behavior is very unusual in HDS measurements.

One possible explanation for such a peaklike feature is that it is due to some kind of short-range ordering, for example, a superlattice modulation of the FeTe layers, or a short-range clustering of the excess Fe itself [though we note that such a clustering scenario appears to be ruled out by scanning tunneling spectroscopy experiments[15]]. One argument against this picture is that the wave vector seems quite arbitrary and does not correspond to any particular symmetry of the crystal structure. Rather, the "peaks" occur exactly along the ridge of maximum Huang diffuse scattering—which seems to suggest that a more likely explanation is that the peak is also coming from the excess Fe-induced strain field and is not some kind of ordering. Further, the peak structure shows little, if any, dependence on the excess Fe concentration (Fig. 1), which would be difficult to explain were it due to a clustering of the excess Fe. Finally, and perhaps most conclusively, the temperature dependence of the scattering, discussed in detail below, shows that the peaklike features and the HDS intensity close to the Bragg peaks have identical behavior—specifically both exhibit a sudden jump at T_N. This again points to a common origin to the scattering. We conclude that the peaklike feature is, in fact, a feature of the Huang diffuse scattering and not a signature of short-range ordering.

To understand how strain fields can produce such a peak, we must first review the theory of HDS. The presence of excess Fe in the crystal causes "extra" forces—known as Kanzaki forces[16]—which distort the structure and give rise to long-range strain. This excess Fe-induced strain field, which breaks the crystal translational symmetry, gives rise to diffuse scattering tails which extend from fundamental Bragg peaks—the Huang diffuse scattering. Within a harmonic approximation, which assumes that the lattice distortion is a linear response to the Kanzaki force, the HDS intensity resulting from the presence of uncorrelated defects can be written as[14,17]

$$I_{\mathrm{HDS}} = x(1-x)\left|\sum_{k\alpha} \tilde{f}_k e^{i\vec{G}\cdot\vec{R}_k} Q_\alpha \sum_{j\beta} \frac{e_{k\alpha}(\vec{q}\,j) e^*_{k'\beta}(\vec{q}\,j)}{\omega^2_{\vec{q}\,j}\sqrt{M_k M_{k'}}} \times \sum_{l'k'} F_{l'k'\beta} e^{-i\vec{q}\cdot\vec{R}_{l'k'}}\right|^2, \quad (1)$$

where x is the defect level (in this case, the extra Fe concentration), and l' and (k, k') are the unit cell index and the atomic index within a unit cell, respectively. The eigenvector and eigenvalue for the jth phonon mode at reduced wave vector transfer $\vec{q} = \vec{Q} - \vec{G}$ are $\vec{e}_k$ and ω, respectively, and $\vec{Q}$ is the total momentum transfer. Indices α, β run over x, y, z. The last summation is over all the Kanzaki forces $\vec{F}_{l'k'}$ exerted on atoms $l'k'$ that are $\vec{R}_{l'k'}$ away from the defect. The phonon eigenvectors and eigenvalues are known parameters, which can be obtained by other means. In our simulation discussed below, they are calculated by using the linear response method implemented by ABINIT code[18] within a local density approximation of density-functional theory. Thus, the Huang diffuse scattering intensity measures the forces between the defect and its surrounding atoms in a summed way.

In most cases, only the Kanzaki forces on the very closest neighbors are significant. Thus, $|\vec{R}_{l'k'}|$ is small and $e^{-i\vec{q}\cdot\vec{R}_{l'k'}}$ can be approximated by $1 - i\vec{q}\cdot\vec{R}_{l'k'}$. As a result, the HDS intensity becomes monotonic and proportional to $1/q^2$.[17] The fact that in the present data, the HDS from $Fe_{1+x}Te$ starts to deviate from a monotonic dependence even at small

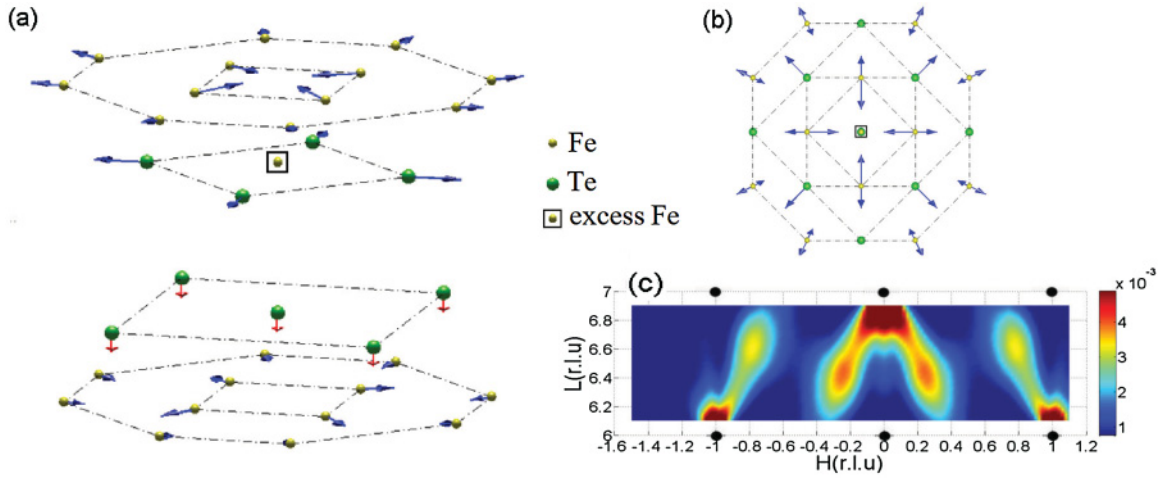

FIG. 2. (Color online) Simulation of Huang diffuse scattering intensity. (a), (b) Top and side views, respectively, for the force pattern used in the simulation. The direction and the length of the arrows indicate the direction and amplitude of the forces. The lengths of the down-pointing arrows (red) in (a) are amplified by a factor of 5 to be visible. Dashed lines indicate the coordination shells with respect to the excess Fe in the Fe2 site. (c) The calculated intensity in the $(H0L)$ plane resulting from this force pattern.

$q \sim (0.1,0,0.2)$ strongly suggests that the first-order approximation for the $e^{-i\vec{q}\cdot\vec{R}_{l'k'}}$ term has broken down and the Kanzaki forces on the atoms far from the excess Fe sites are also significant. That is, the interaction of the excess Fe with FeTe layers has an effect that extends across several FeTe unit cells.

To demonstrate that extended Kanzaki forces can account for the observed HDS pattern, we have carried out a simulation of the HDS scattering that results from extending the Kanzaki forces to the second and third nearest unit cells. We have assumed tetragonal symmetry in this modeling, although the low temperature monoclinic/orthorhombic phases of $Fe_{1+x}Te$ are of lower symmetry. This simplification is valid because our data averages over the contribution from the different domains at low temperature, and is further justified by the fact that the orthorhombic/monoclinic splitting is fairly small(∼1%), compared to the width of the features observed in diffuse scattering.

The force pattern in our model, together with the resulting scattered intensity, is shown in Fig. 2. One observes the same characteristic pattern as seen in the experimental data. We can now see that the peak arises from the phase factors of Eq. (1) and, in particular, the interference between the forces in different neighboring shells. While the precise details of the intensity and distribution depend on the particular values of the forces chosen, we find that this peaklike structure is a robust consequence of extending the forces beyond the nearest neighbors. In principle, one could now go further and carry out a quantitative fitting of the data, as was done in the case of $La_{1.2}Sr_{1.8}Mn_2O_7$ (Ref. 14) to obtain the values of these forces. However, the large number of Kanzaki forces in the present case makes it very difficult to ensure such fits are unique. To avoid misleading the reader, we, therefore, do not reproduce the details of the forces producing the pattern in Fig. 2 here. The important point is that by extending the effect of the excess Fe to beyond nearest neighbors, the natural interferences give rise to the nonmonotonic scattering observed in the experiments, and that, therefore, these peaks are a direct signature of the extended nature of the forces and resulting large strain field, arising from the excess Fe in the crystal structure.

Microscopically, it is unlikely that such a strong long-range response of the lattice originates from the Coulomb force introduced by the excess Fe, given the efficient screening present in this system as a result of the metallic carriers. Instead, we argue that it reflects the correlated nature of the electronic structure in FeTe. Recall[19] that the effective interactions between the Fe atoms within the layers are predominantly superexchange in the spin and orbital channels via kinetic processes through the intermediate Te-p orbitals. These superexchange processes are easily modified by the excess Fe, which can change the p-orbital energy through a shift in the positions of the Te atoms surrounding the excess Fe. Further, since the Fe-orbital degree of freedom is also coupled via these same superexchange paths, a strong lattice response is also to be expected. Indeed, the large anharmonic forces deduced above are acting precisely on those Fe atoms connected by the Te atoms surrounding the excess Fe [Fig. 2(a)]. In short, our observed anomalous long-range response in Kanzaki forces testifies to the strongly correlated orbital and spin structure in FeTe.

We now turn to the temperature dependence of the diffuse scattering. This was measured for the $x = 0.03$ and $x = 0.08$ samples, for which T_N was determined from magnetic susceptibility measurements to be 67 and 59 K, respectively. H scans at several L values were measured as a function of temperature. Figures 3(a) and 3(c) show scans collected at temperatures near T_N for each sample. In both samples, an abrupt jump in the diffuse intensity is seen in the vicinity of the respective phase transitions for all L values measured.

In the lower two panels of Fig. 3, we plot difference curves. For each sample, a baseline scan is chosen, well below T_N (specifically, $T = 60$ K for $x = 0.03$ and $T = 52$ K for $x = 0.08$). For data taken above this baseline temperature, but below T_N, only a smooth featureless increase is observed (red curves with open circles). This increase is due to the thermal diffuse scattering. However, for data taken right

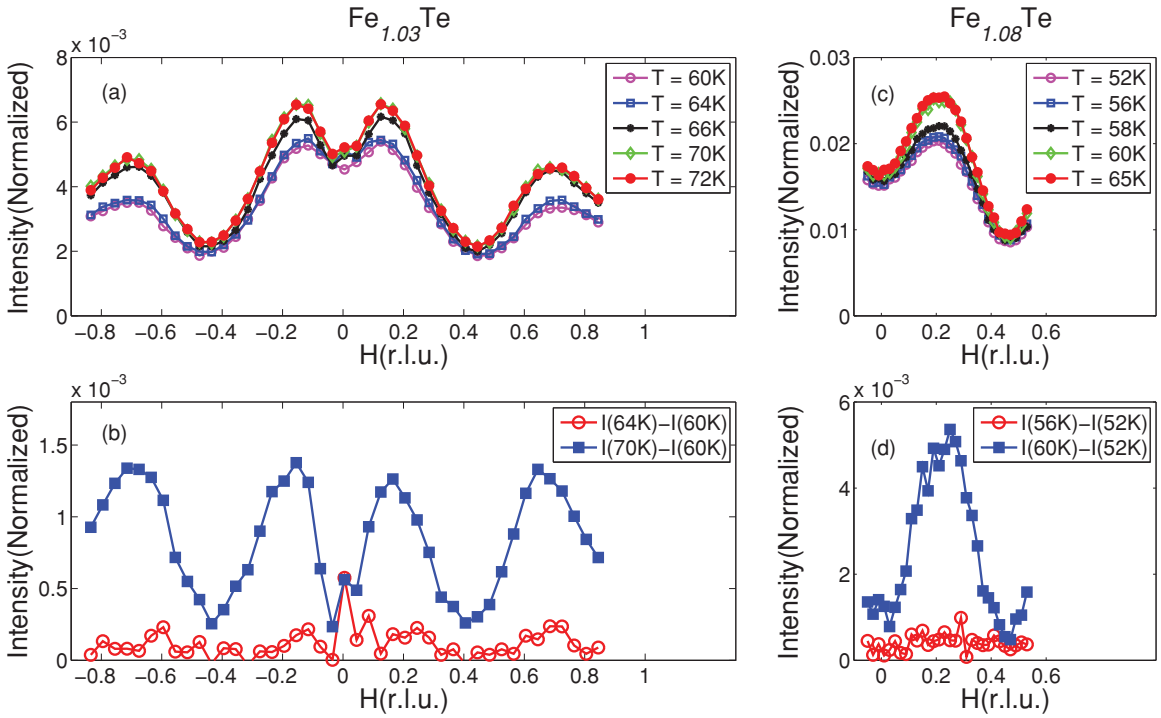

FIG. 3. (Color online) (a), (c) H scans as a function of temperature near T_N for $Fe_{1.03}Te$ (taken at $L = 6.7$) and $Fe_{1.08}Te$ (taken at $L = 6.6$). (b), (d) Difference curves for the scattered intensity with respect to the lowest temperature shown in each case, for temperatures just below (red curves with open circles) and just above (blue curves with solid squares) T_N for each sample.

above T_N (blue curves with solid squares), a large increase is seen relative to the baseline. Further, the q-dependence of the increase mirrors that of the HDS itself. Thus, the increase in diffuse intensities across T_N arises from the HDS and not from other thermal effects.

In Fig. 4, the temperature dependence of the diffuse intensity from the two samples at selected Q points is plotted. The intensities were normalized to be unity just before the increase in each case. At Q_1 and Q_2, which are close to [0 0 7], the intensity jump is about 20% for both samples. Aside from this abrupt jump at T_N, the diffuse intensities at these Q points show an approximately linear temperature dependence, which likely reflects the temperature dependence of the underlying thermal diffuse scattering (TDS). We also show the temperature dependence at $Q_3 = (0.68\ 0\ 6.7)$, far from any strong Bragg peaks for $Fe_{1.03}Te$, where the contribution from such TDS is expected to be small. At Q_3, the linear temperature dependence disappears, suggesting the TDS is, indeed, negligible here. The diffuse intensity is then predominantly HDS, together with a constant background, and the jump at T_N is now seen to be close to 40%. By assuming the TDS is proportional to temperature and that the HDS is temperature independent above and below the transition, the amplitude of the jump for HDS can be estimated to be 30% for $Fe_{1.08}Te$ at Q_1 and 38% for $Fe_{1.03}Te$ at Q_2, and thus we conclude that there is a large increase in the HDS throughout the Brillouin zone at T_N.

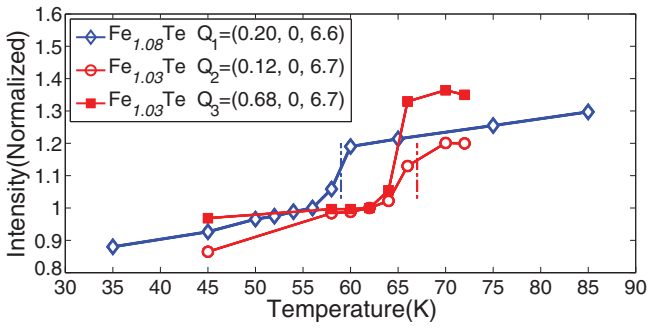

FIG. 4. (Color online) Temperature dependence of the HDS intensities from $Fe_{1.03}Te$ (red curves with open circles and solid squares) and $Fe_{1.08}Te$ (blue curve with open diamonds) as measured at different Q points. The dashed lines indicate T_N for the two samples.

This dramatic change in HDS can either occur due to a change in the Kanzaki forces themselves, or to a change in the lattice response to those forces—due to a structural phase transition. This latter would be manifest as a change in the phonon frequencies and, hence, affect the HDS through Eq. (1). In order to reproduce the observed significant change in the HDS entirely through such changes in the phonon spectra, then ω would need to be hardened by ~8% on cooling through T_N. Further, Fig. 3 shows that the intensity jump occurs throughout the Brillouin zone. Thus, any such hardening must be a general feature of the entire phonon spectrum and not restricted to a single mode. It would, therefore, show up in the phonon density of states measurements as a general shift of the spectrum across T_N. Such phonon measurements are not presently available for $Fe_{1+x}Te$. However, they have been made on another chalcogenide, FeSe,[20,21] and also on the related pnictides.[22] These measurements show that the structural or magnetic phase transition has little effect on the phonon dynamics. Thus, we conclude that the change in the HDS

intensity observed here at T_N must be due to change in the Kanzaki forces.

We have argued that the observed strong lattice response is unlikely to originate from the Coulomb force introduced by the excess Fe. The temperature dependence of the HDS further supports this argument. The Coulomb interaction scenario would require a change in the charge state of the Fe atoms across T_N to explain the observed intensity change. In fact the Hall coefficient has been observed to change in $Fe_{1+x}Te$ across T_N.[8,9] However, this change depends strongly on the excess Fe concentration, and a much larger Hall coefficient change is observed on samples with smaller Fe2 concentrations.[9] In contrast, the HDS intensity jump at T_N that we observed shows a similar amplitude for $x = 0.03$ and 0.08, and we, therefore, argue that the change observed in the Hall effect measurements is not connected with the changes observed in our HDS measurements.

The observed dramatic drop in the HDS indicates an abrupt reduction of the lattice response to the excess Fe. We argue that again this is an electronic effect and that it reflects the first-order change of the electronic structure of FeTe across T_N.[23] Specifically, upon reducing the temperature across the orbital/spin transition, the system orders and locks into a particular combination of orbitals and spins. Obviously, with the freedoms in the orbital and spin channels now removed, the total energy cost of any lattice distortion increases because of the additional electronic energy price that must now be paid. Thus, the system becomes more rigid and less able to respond to the excess Fe. Interestingly, since the measured HDS is a measure of the very local response, the significant drop in the HDS intensity across the transition temperature indicates a very strong change in the local electronic structure, suggesting that the local change may be larger than the average, long-range change given by the long-range order parameter of the crystal structure.

In conclusion, we have carried out single crystal x-ray diffuse scattering measurements of $Fe_{1+x}Te$. Strong diffuse scattering is observed with a characteristic (modulated) momentum dependence, indicative of a large excess Fe-induced local lattice distortion. The unusual momentum dependence implies that the interactions between excess Fe with FeTe layers extend over several unit cells. The strength and the extended nature of the interaction suggests that this is the mechanism through which the excess Fe stabilizes the overall crystal structure.

More importantly, unlike defects in other systems which are introduced for doping purposes and may otherwise be regarded as inactive, the strong and unique response of the FeTe layer to the excess Fe and its significant coupling to the structural and magnetic phase transition allow us to use the excess Fe as an intrinsic local probe of the FeTe system. Both the extended nature of the interaction between excess Fe and FeTe layers and its temperature dependence testify to the strongly correlated orbital and spin structure in FeTe.

Finally, given the experimental observations of doping dependence of the Neel temperature and the magnetic wave vector, we suggest that the distortions observed here are significant in determining the properties of these all-important FeTe layers and should be taken into account in future attempts to understand these materials.

This work at Brookhaven was supported by the US Department of Energy, Division of Materials Science, under Contract No. DE-AC02-98CH10886.

[1] A. Subedi, L. Zhang, D. J. Singh, and M.-H. Du, Phys. Rev. B **78**, 134514 (2008).
[2] S. Li, C. de la Cruz, Q. Huang, Y. Chen, J. W. Lynn, J. Hu, Y.-L. Huang, F.-C. Hsu, K.-W. Yeh, M.-K. Wu, and P. Dai, Phys. Rev. B **79**, 054503 (2009).
[3] W. Bao, Y. Qiu, Q. Huang, M. A. Green, P. Zajdel, M. R. Fitzsimmons, M. Zhernenkov, S. Chang, M. H. Fang, B. Qian, E. K. Vehstedt, J. H. Yang, H. M. Pham, L. Spinu, and Z. Q. Mao, Phys. Rev. Lett. **102**, 247001 (2009).
[4] D. Fruchart, P. Convert, P. Wolfers, R. Madar, J. P. Senateur, and R. Fruchart, Mater. Res. Bull. **10**, 169 (1975).
[5] M. J. Pitcher, D. R. Parker, P. Adamson, S. J. C. Herkelrath, A. T. Boothroyd, R. M. Ibberson, M. Brunelli, and S. J. Clarke, Chem. Commun. **45**, 5918 (2008).
[6] L. Zhang, D. J. Singh, and M. H. Du, Phys. Rev. B **79**, 012506 (2009).
[7] Z. Xu, J. Wen, G. Xu, Q. Jie, Z. Lin, Q. Li, S. Chi, D. K. Singh, G. Gu, and J. M. Tranquada, Phys. Rev. B **82**, 104525 (2010).
[8] G. F. Chen, Z. G. Chen, J. Dong, W. Z. Hu, G. Li, X. D. Zhang, P. Zheng, J. L. Luo, and N. L. Wang, Phys. Rev. B **79**, 140509(R) (2009).
[9] T. J. Liu, X. Ke, B. Qian, J. Hu, D. Fobes, E. K. Vehstedt, H. Pham, J. H. Yang, M. H. Fang, L. Spinu, P. Schiffer, Y. Liu, and Z. Q. Mao, Phys. Rev. B **80**, 174509 (2009).
[10] H. C. Lei, R. W. Hu, E. S. Choi, J. B. Warren, and C. Petrovic, Phys. Rev. B **81**, 184522 (2010).
[11] K. Huang, Proc. R. Soc. London A **190**, 102 (1947); P. H. Dederichs, J. Phys. F **3**, 471 (1973).
[12] Z. Islam, X. Liu, S. K. Sinha, J. C. Lang, S. C. Moss, D. Haskel, G. Srajer, P. Wochner, D. R. Lee, D. R. Haeffner, and U. Welp, Phys. Rev. Lett. **93**, 157008 (2004).
[13] W. Dmowski, R. J. McQueeney, T. Egami, Y. P. Feng, S. K. Sinha, T. Hinatsu, and S. Uchida, Phys. Rev. B **52**, 6829 (1995).
[14] B.J. Campbell, S. K. Sinha, R. Osborn, S. Rosenkranz, J. F. Mitchell, D. N. Argyriou, L. Vasiliu-Doloc, O. H. Seeck, and J. W. Lynn, Phys. Rev. B **67**, 020409(R) (2003).
[15] T. Kato, Y. Mizuguchi, H. Nakamura, T. Machida, H. Sakata, and Y. Takano, Phys. Rev. B **80**, 180507(R) (2009).
[16] H. Kanzaki, J. Phys. Chem. Solids. **2**, 24 (1957).
[17] M. A. Krivoglaz, *X-Ray and Neutron Diffraction in Nonideal Crystals* (Springer, Berlin, 1996).

[18]X. Gonze, J. M. Beuken, R. Caracas, F. Detraux, M. Fuchs, G. M. Rignanese, L. Sindic, M. Verstraete, G. Zerah, F. Jollet, M. Torrent, A. Roy, M. Mikami, Ph. Ghosez, J.-Y. Raty, and D. C. Allan, Comput. Mater. Sci. **25**, 478 (2002).

[19]F. Ma, W. Ji, J. Hu, Z.-Y. Lu, and T. Xiang, Phys. Rev. Lett. **102**, 177003 (2009); C. C. Lee, W. G. Yin, and W. Ku, *ibid.* **103**, 267001 (2009); C.-Y. Moon and H. J. Choi, *ibid.* **104**, 057003 (2010).

[20]D. Phelan, J. N. Millican, E. L. Thomas, J. B. Leao, Y. Qiu, and R. Paul, Phys. Rev. B **79**, 014519 (2009).

[21]V. Ksenofontov, G. Wortmann, A. I. Chumakov, T. Gasi, S. Medvedev, T. M. McQueen, R. J. Cava, and C. Felser, Phys. Rev. B **81**, 184510 (2010).

[22]O. Delaire, M. S. Lucas, A. M. dos Santos, A. Subedi, A. S. Sefat, M. A. McGuire, L. Mauger, J. A. Munoz, C. A. Tulk, Y. Xiao, M. Somayazulu, J. Y. Zhao, W. Sturhahn, E. E. Alp, D. J. Singh, B. C. Sales, D. Mandrus, and T. Egami, Phys. Rev. B **81**, 094504 (2010).

[23]Y. Zhang, F. Chen, C. He, L. X. Yang, B. P. Xie, Y. L. Xie, X. H. Chen, M. Fang, M. Arita, K. Shimada, H. Namatame, M. Taniguchi, J. P. Hu, and D. L. Feng, Phys. Rev. B **82**, 165113 (2010).